

# PARALLEL 3D FINITE ELEMENT PARTICLE-IN-CELL SIMULATIONS WITH Pic3P\*

A. Candel<sup>†</sup>, A. Kabel, L. Lee, Z. Li, C. Ng, G. Schussman and K. Ko,  
SLAC, Menlo Park, CA 94025, U.S.A.

I. Ben-Zvi, J. Kewisch,  
BNL, Upton, NY 11973, U.S.A.

## Abstract

SLAC's Advanced Computations Department (ACD) has developed the parallel 3D Finite Element electromagnetic Particle-In-Cell code Pic3P. Designed for simulations of beam-cavity interactions dominated by space charge effects, Pic3P solves the complete set of Maxwell-Lorentz equations self-consistently and includes space-charge, retardation and boundary effects from first principles. Higher-order Finite Element methods with adaptive refinement on conformal unstructured meshes lead to highly efficient use of computational resources. Massively parallel processing with dynamic load balancing enables large-scale modeling of photoinjectors with unprecedented accuracy, aiding the design and operation of next-generation accelerator facilities. Applications include the LCLS RF gun and the BNL polarized SRF gun.

## THE PARALLEL CODE Pic3P

In Pic3P, the full set of Maxwell's equations is solved numerically in time domain using parallel higher-order Finite Element methods. Electron macro-particles are pushed self-consistently in space charge, wake- and external drive fields.

### Finite Element Time-Domain Field Solver

Ampère's and Faraday's laws are combined and integrated over time to yield the inhomogeneous vector wave equation for the time integral of the electric field  $\mathbf{E}$ :

$$\left( \varepsilon \frac{\partial^2}{\partial t^2} + \sigma \frac{\partial}{\partial t} + \nabla \times \mu^{-1} \nabla \times \right) \int^t \mathbf{E}(\mathbf{x}, \tau) d\tau = -\mathbf{J}(\mathbf{x}, t), \quad (1)$$

with permittivity  $\varepsilon$  and permeability  $\mu$ . The effective conductivity  $\sigma$  provides a simple model for damping in lossy materials.

The computational domain is discretized into curved tetrahedral elements and  $\int^t \mathbf{E} d\tau$  in Equation (1) is expanded into a set of hierarchical Whitney vector basis functions  $\mathbf{N}_i(\mathbf{x})$  up to order  $p$  within each element:

$$\int^t \mathbf{E}(\mathbf{x}, \tau) d\tau = \sum_{i=1}^{N_p} e_i(t) \cdot \mathbf{N}_i(\mathbf{x}). \quad (2)$$

\* Work supported by the U. S. DOE ASCR, BES, and HEP Divisions under contract No. DE-AC002-76SF00515.

<sup>†</sup> candel@slac.stanford.edu

Substituting Equation (2) into Equation (1), multiplying by a test function and integrating over the computational domain results in a system of linear equations (second-order in time) for the coefficients  $e_i$ . Numerical integration is performed with the unconditionally stable implicit Newmark-Beta scheme [1]. More detailed information about the employed methods has been published earlier [2].

### Higher-Order Particle-Field Coupling

Electron macro particles are specified by position  $\mathbf{x}$ , momentum  $\mathbf{p}$ , rest mass  $m$  and charge  $q$ . The total current density  $\mathbf{J}$  in Equation (1) is then approximated as

$$\mathbf{J}(\mathbf{x}, t) = \sum_i q_i \cdot \delta(\mathbf{x} - \mathbf{x}_i(t)) \cdot \mathbf{v}_i(t), \quad (3)$$

with  $\mathbf{v} = \frac{\mathbf{p}}{\gamma m}$ ,  $\gamma^2 = 1 + |\frac{\mathbf{p}}{mc}|^2$ . The classical relativistic collision-less Newton-Lorentz equations of motion are integrated using the standard Boris pusher [3].

Starting with correct initial conditions and fulfilling the discrete versions of Equation (1) and the continuity equation

$$\frac{\partial \rho}{\partial t} + \nabla \cdot \mathbf{J} = 0 \quad (4)$$

simultaneously during time integration leads to numerical charge conservation.

The use of higher-order finite elements not only significantly improves field accuracy and dispersive properties [4], but also leads to intrinsic higher-order accurate particle-field coupling.

### Causal Moving Window and Load Balancing

Pic3P has been optimized for high efficiency both on workstations as well as large supercomputers.

Computations can be restricted to the causal field region around the particle bunch without any loss of accuracy. This 'moving window' feature of Pic3P can save orders of magnitude in memory and CPU time requirements and allows full EM 3D PIC simulations on desktop computers [5].

Dynamic load balancing allows the solution of large problems with hundreds of millions of field degrees of freedom (DOFs) and billions of particles and enables unprecedented accuracy in self-consistent state-of-the-art simulations of beam-cavity interactions.

Figure 1 shows field and particle partitioning among different CPUs for efficient load balancing. Both memory and speed scalability has been optimized.

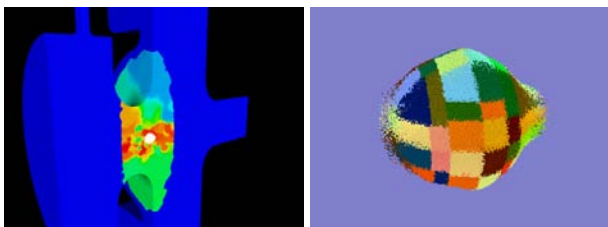


Figure 1: Parallel dynamic load balancing in Pic3P is achieved by partitioning the fields and particles differently and optimizing the required communication between processors. Colors indicate ownership by processors of fields (left) and particles (right). The field calculation is restricted to the causal moving window for improved efficiency.

## VALIDATION: LCLS RF GUN

PIC simulations of the 1.6-cell S-band LCLS RF gun are presented [6]. Simulation parameters are:  $\pi$ -mode, 120 MV/m, 1 nC, 10 ps, 1 mm beer-can initial bunch distribution, centroid injection phase  $-58^\circ$  and no solenoid. These parameters allow comparisons between the 3D results from simulations with Pic3P and PARMELA and the 2D results from simulations with Pic2P and MAFIA.

Figure 2 shows a comparison of transverse emittance results by the different codes. For Pic3P simulations, a con-

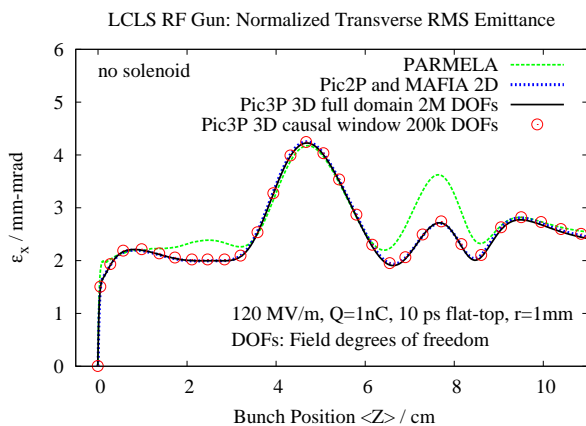


Figure 2: Comparison of normalized transverse RMS emittance as a function of beam position in the LCLS RF gun as calculated with PARMELA, Pic2P and MAFIA 2D (both agree), and Pic3P, where the causal moving window technique reduces the problem size by one order of magnitude.

formal, unstructured 3D (1/4) mesh model with 305k tetrahedral elements is used, with mesh refinement along the center of the beam pipe. High fidelity cavity mode fields are obtained with the parallel Finite Element frequency do-

main code Omega3P and directly loaded into Pic3P as drive fields.

Excellent agreement between 3D results from Pic3P and the 2D results from Pic2P is found, as expected from the high cylindrical symmetry in the fields, as well as perfect agreement with MAFIA 2D as expected from the convergence behavior of the codes. PARMELA results differ as space-charge effects are significant, presumably because wakefield and retardation effects are ignored, as detailed in a previous study [2]. Simulation results starting from a measured initial bunch distribution have been published earlier [5].

## BNL POLARIZED SRF GUN

An ongoing experiment at BNL investigates the use of a superconducting RF gun to provide polarized, high-brightness electron beams for the ILC without the need for a damping ring [7]. Key limiting factors include the vacuum quality ( $10^{-12}$  Torr), cathode (GaAs-type) characteristics and the ability to shape the initial bunch distribution.

The parameters are: 1/2-cell, 350 MHz, 24.5 MV/m gradient, solenoid field of 18 Gauss at the cathode, 3.2 nC bunch charge, cathode spot size 6.5 mm, centroid injection at  $-42.5^\circ$  before crest and a bunch length of 220 ps. The initial bunch shape is a combination of two ellipsoids obtained from a parametric optimization for lowest emittance as predicted with the code PARMELA.

Figure 3 shows a snapshot of the bunch and the scattered self-fields from a simulation with Pic3P that includes all space charge and wakefield effects.

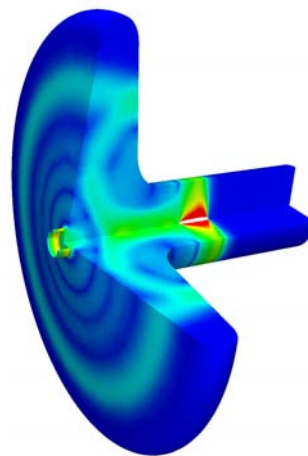


Figure 3: Snapshot of bunch and scattered self-fields in the BNL polarized SRF gun, as simulated with Pic3P.

In the following, a comparison of PARMELA and Pic3P results is shown. Both codes use the same initial particle distribution and the same field maps.

Figure 4 shows a comparison of the transverse phase space in the zero space charge limit – agreement is found.

Figures 5 and 6 show the transverse phase space and emittance for simulations with a bunch charge of 3.2 nC.

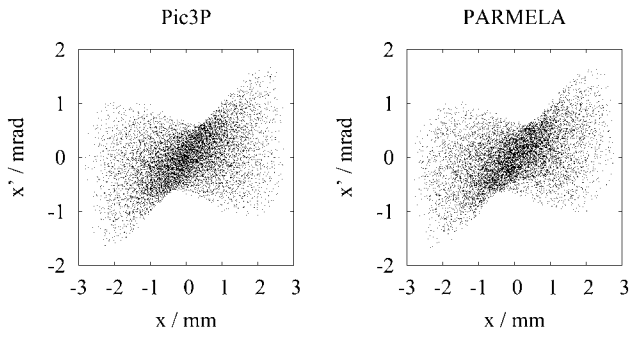


Figure 4:  $x - x'$  trace space of the particle bunch at an observer plane at  $Z=19$  cm, as calculated with Pic3P and PARMELA in the zero space charge limit.

All other parameters are kept the same as for the previous calculations in the zero space charge limit.

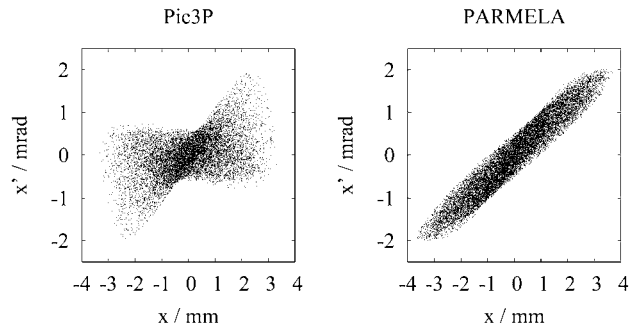


Figure 5:  $x - x'$  trace space of the particle bunch at an observer plane at  $Z=19$  cm, as calculated with Pic3P and PARMELA for a bunch charge of 3.2 nC.

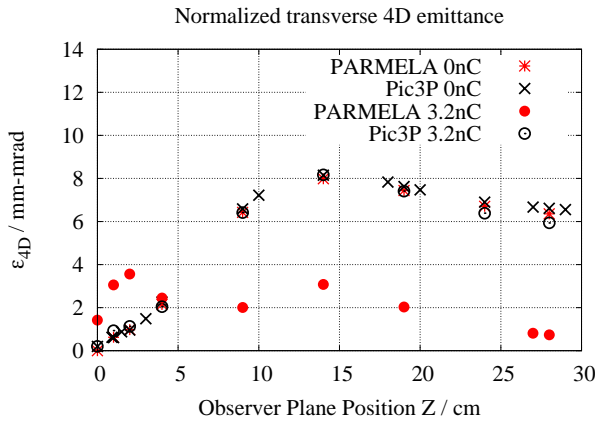


Figure 6: Comparison of 4D emittance results by PARMELA and Pic3P, where  $\epsilon_{4D} := \sqrt[4]{\det(\sigma)}$ ,  $\sigma_{ij} = \langle (\zeta_i - \langle \zeta_i \rangle) (\zeta_j - \langle \zeta_j \rangle) \rangle$ , and  $\zeta = \{x, y, \gamma\beta_x, \gamma\beta_y\}$ .

The differences between PARMELA and Pic3P results are expected to stem from the different space charge models, but further study will be required to determine the exact cause for the discrepancy. It is expected that Pic3P emit-

tance calculations will result in a different set of optimal operating parameters, as wakefield and retardation effects are included in the simulations.

## SUMMARY

SLAC has developed the first high-performance higher-order 3D Finite Element PIC code Pic3P, for realistic modeling of low energy, space-charge dominated beam-cavity interactions. State-of-the-art parallel Finite Element methods on conformal, unstructured meshes in combination with moving window techniques and dynamic load balancing enable efficient simulations of low-emittance electron injectors with unprecedented accuracy. Pic3P has been thoroughly validated and applied for emittance calculations for the LCLS RF gun and the BNL polarized SRF gun and fast solution convergence is achieved, while results by the electrostatic code PARMELA show some differences.

## ACKNOWLEDGMENTS

This work was supported by the US DOE ASCR, BES, and HEP Divisions under contract No. DE-AC002-76SF00515. This research used resources of the National Energy Research Scientific Computing Center, and of the National Center for Computational Sciences at Oak Ridge National Laboratory, which are supported by the Office of Science of the U. S. Department of Energy under Contract No. DE-AC02-05CH11231 and No. DE-AC05-00OR22725. – We also acknowledge the contributions from our SciDAC collaborators in numerous areas of computational science.

## REFERENCES

- [1] N. M. Newmark, “A method of computation for structural dynamics”, Journal of Eng. Mech. Div., ASCE, vol. 85, pp. 67-94, July 1959.
- [2] A. Candel et al., “Parallel Higher-order Finite Element Method for Accurate Field Computations in Wakefield and PIC Simulations”, Proc. ICAP 2006, Chamonix Mont-Blanc, France, Oct. 2-6, 2006.
- [3] J. P. Boris, “Relativistic plasma simulation-optimization of a hybrid code”, Proc. Fourth Conf. Num. Sim. Plasmas, Naval Res. Lab, Wash. D.C., pp. 3-67, Nov. 2-3, 1970.
- [4] M. Ainsworth, “Dispersive properties of high-order Nedelec/edge element approximation of the time-harmonic Maxwell equations”, Philos. trans.-Royal Soc., Math. phys. eng. sci., vol. 362, no. 1816, pp. 471-492, 2004.
- [5] A. Candel et al, “High-Fidelity RF Gun Simulations with the Parallel 3D Finite Element Particle-In-Cell Code Pic3P”, Proc. Workshop on Polarized Electron Sources, Jefferson Lab, Oct 1-3, 2008
- [6] L. Xiao et al., “Dual Feed RF Gun Design for the LCLS”, Proc. PAC 2005, Knoxville, Tennessee, May 15-20, 2005.
- [7] J. Kewisch et al, “The Polarized SRF Gun Experiment”, POLARIZED ION SOURCES, TARGETS AND POLARIMETRY - PSTP2007: 12th International Workshop. AIP Conf. Proc., vol. 980, pp. 118-123, 2008